Communication

Bacterial Aerobic Synthesis of Nanocrystalline Magnetite

Atul Bharde, Aijaz Wani, Yogesh Shouche, Pattayil A. Joy, Bhagavatula L. V. Prasad, and Murali Sastry

J. Am. Chem. Soc., **2005**, 127 (26), 9326-9327• DOI: 10.1021/ja0508469 • Publication Date (Web): 09 June 2005

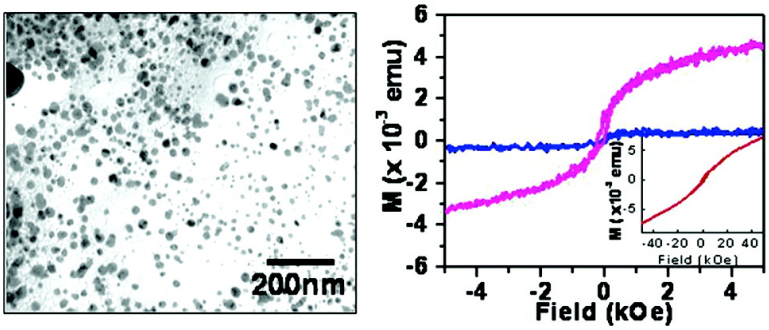

More About This Article

Additional resources and features associated with this article are available within the HTML version:

- Supporting Information
- Links to the 11 articles that cite this article, as of the time of this article download
- Access to high resolution figures
- Links to articles and content related to this article
- Copyright permission to reproduce figures and/or text from this article

View the Full Text HTML

J|A|C|S
COMMUNICATIONS

Published on Web 06/09/2005

Bacterial Aerobic Synthesis of Nanocrystalline Magnetite

Atul Bharde,[†] Aijaz Wani,[‡] Yogesh Shouche,[‡] Pattayil A. Joy,[†] Bhagavatula L. V. Prasad,[†] and Murali Sastry*,[†]

Nanoscience Group, Materials Chemistry Division, National Chemical Laboratory, Pune 411 008, India, and Molecular Biology Unit, National Center for Cell Science, Pune 411 007, India

Received February 9, 2005; E-mail: sastry@ems.ncl.res.in

Oxide nanoparticles are important in applications such as catalysis,[1] electronics,[2] and anti-microbial coatings.[3] Interest in the synthesis of iron oxide nanoparticles, especially magnetite, has centered on applications such as multi-terabit magnetic storage devices,[4] ferrofluids,[5] MRI contrast enhancement agents,[6] and separation processes.[7] Chemical methods for preparing magnetic iron oxide nanoparticles are energy intensive, employ toxic chemicals, and often yield particles in nonpolar organic solutions,[8] thus precluding biomedical application. In contrast, biological magnetite synthesis occurs in water at room temperature and close to neutral pH. Laboratory studies on magnetite growth have focused exclusively on the use of magnetotactic bacteria[9−12] and iron-reducing bacteria, such as *Geobacter metallireducens* (a distant cousin of magnetotactic bacteria).[13] In all studies to date, biosynthesis of magnetite was found to be extremely slow (often requiring 1 week) under strictly anaerobic conditions. We report our discovery that the bacterium *Actinobacter* spp. is capable of magnetite synthesis by reaction with suitable aqueous iron precursors under fully aerobic conditions. The magnetite nanoparticles form extracellularly and show excellent magnetic properties.

The aerobic bacterium *Actinobacter* spp. was isolated as a contaminant from a flask containing an aqueous mixture of potassium ferricyanide/ferrocyanide that had been stored in air for 2 weeks (experimental details in Supporting Information, S1). Magnetite is formed within 24 h by reaction of *Actinobacter* spp. with an aqueous potassium ferricyanide/ferrocyanide mixture under fully aerobic conditions, thus considerably simplifying the synthetic procedure. The pH of the $K_3Fe(CN)_6/K_4Fe(CN)_6$ reaction medium was adjusted to 6.4 using diluted HCl and was measured to be 6.6 at the end of reaction with *Actinobacter* spp. The bacterium was identified using the molecular phylogenic method of 16S rRNA sequencing. The 16S rRNA sequence showed maximum similarity with *Actinobacter* strain EC5 when analyzed by the BLAST at NCBI program (Supporting Information, S1). The region of the 16S rRNA gene used for analysis gives reliable information about phylogenetic affiliation.[14] Further analysis using the Dnadist program showed maximum similarity (98.2%) with *Actinobacter* strain EC5 (NCBI genebank accession no. AY 337600) and thus could be assigned to the genus *Actinobacter* (NCBI genebank accession no. AY 864333).

Representative transmission electron microscopy (TEM) images of iron oxide nanoparticles formed after 24 and 48 h in the bacterium−$K_3Fe(CN)_6/K_4Fe(CN)_6$ reaction medium are shown in Figure 1A and C, respectively. After 24 h, a high percentage of quasi-spherical nanoparticles of 10−40 nm are obtained. The selected area diffraction (SAED) analysis of the spherical iron oxide nanoparticles indicates that they are crystalline (Figure 1B); the diffraction spots could be indexed on the basis of the structure of magnetite. After 48 h of reaction, uniform cubic particles of 50−150 nm edge lengths (Figure 1C and inset) are observed. The number of spherical particles is much reduced, suggesting assembly of the spherical particles into cubic superstructures. At high magnification, one cube reveals voids that could arise from aggregation of smaller spherical nanoparticles (inset, Figure 1C). The magnetite nanoparticle assemblies were stable in solution for weeks, suggesting stabilization of the particles by bioorganic molecules secreted by *Actinobacter* spp. The X-ray diffraction (XRD) pattern recorded from the iron oxide powder after 48 h of reaction shows strong Bragg reflections that could be indexed based on a mixed γ-Fe_2O_3 [maghemite; ○ peaks; *d*-values 2.02 (410), 1.63 (510)] and Fe_3O_4 [magnetite; ▲ peaks; *d*-values: 2.86 (220), 2.44 (311), 2.02 (400), 1.26 (622), 0.96 (642)] phase (Figure 2A, red curve).[15]

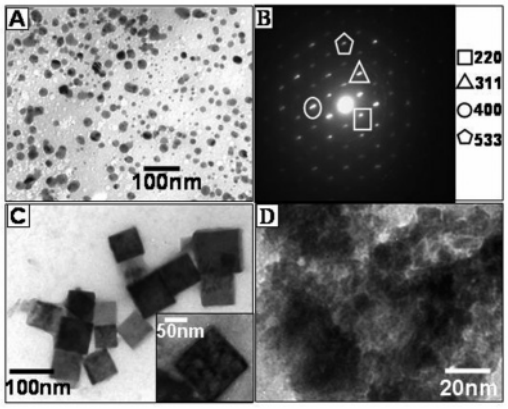

Figure 1. (A) TEM image of magnetite nanoparticles after 24 h of reaction with *Actinobacter* spp. (B) SAED pattern of the particles in (A). (C and inset) TEM images of magnetite nanoparticles after 48 h of reaction with *Actinobacter* spp. (D) TEM image of the 48 h reacted magnetite nanoparticles after calcination at 350 °C for 3 h.

Fourier transform infrared (FTIR) spectroscopy analysis of centrifuged and purified magnetite nanoparticles after 48 h reaction shows the presence of amide I and II absorption bands due to surface-bound proteins (Figure 2B, △ peaks). In addition, Fe−O vibrational modes are also observed (Figure 2B, ● peaks), indicating hydrolysis of the iron precursors. Thermogravimetric analysis (TGA) of purified powders of magnetite nanoparticles after 48 h of reaction with *Actinobacter* spp. showed a ca. 65% weight loss by 500 °C (Figure 2C) that is attributed to decomposition and desorption of surface-bound proteins. Large changes occur in the nanoparticle morphology after removal of the proteins by calcination at 350 °C (Figure 1D). The cubic assembly of the magnetite nanoparticles is destroyed, and the sintered particles are uniformly dispersed over the grid surface. The XRD pattern recorded from the sintered magnetite particles (blue curve, Figure 2A) is similar to that of the as-prepared particles, indicating that the heat treatment

[†] National Chemical Laboratory.
[‡] National Center for Cell Science.

10.1021/ja0508469 CCC: $30.25

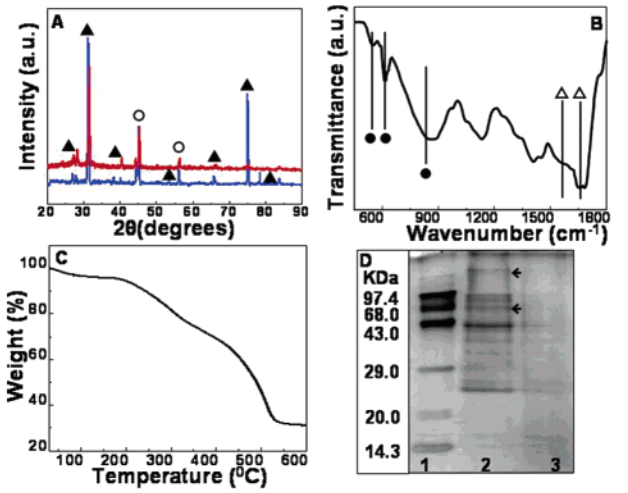

Figure 2. (A) XRD patterns of drop-cast films of iron oxide nanoparticles on glass after reaction with the bacteria for 48 h before (red curve) and after calcination at 350 °C for 3 h (blue curve; see text for details and peak assignments). (B and C) FTIR spectrum and TGA pattern of magnetite nanoparticles after 48 h of reaction of the iron complexes with *Actinobacter* spp., respectively. (D) SDS−PAGE protein profile of the bacterium in the presence (lane 2) and absence (lane 3) of iron salts in solution. The arrows indicate induction of two proteins (lane 2) due to iron salt stress. Lane 1 shows standard protein molecular weight markers.

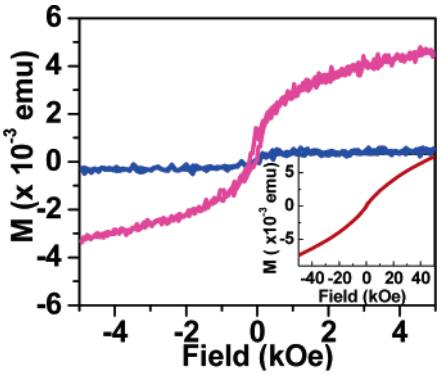

Figure 3. Field dependent magnetization plots of the 48 h reacted biogenic magnetite nanoparticles at 5 K (inset), 300 K (blue curve), and 300 K after calcination (magenta curve).

does not alter the crystallinity and overall composition of the magnetite particles either by way of sintering or by oxidation.

Room temperature (RT) field dependent magnetization measurements of the magnetite nanoparticles obtained after 48 h of reaction with *Actinobacter* spp., before (Figure 3, blue curve) and after calcination for 3 h (magenta curve), indicate that the particles are superparamagnetic in nature. Magnetic particles below a certain size regime exist as single domain particles displaying properties characteristic of superparamagnetism.[8,16,17] The stronger magnetic signal observed from the calcined sample suggests that the high protein content (65 wt %) in the as-prepared particles contributes a large diamagnetic component that reduces the overall magnetization from the as-prepared sample. Further support for this inference comes from the enhanced magnetic signal observed at 5 K from the as-prepared magnetite nanoparticles (inset, Figure 3).

The protein profile of the bacterial biomass obtained in the presence and absence of iron precursors was checked by SDS−PAGE. Exposure of *Actinobacter* spp. to the anionic iron complexes resulted in the induction of two proteins with molecular weights of ca. 120 and 70 kDa (arrows in lane 2, Figure 2D), which are clearly missing in the protein profile obtained from the bacterial culture supernatant when grown in the absence of the iron complexes (lane 3, Figure 2D). The induced proteins were separated by PAGE and together tested for hydrolyzing activity with the iron complexes. Nanoparticles of magnetite were readily obtained by reaction with a mixture of the two proteins (Supporting Information, S2). Magnetite nanoparticles were not obtained by reaction of iron complexes with the proteins secreted by the bacterium grown in the absence of the metal precursors. In yet another control experiment, the aerobic bacteria, *Bacillus subtilis*, *Aerobacter aerogenes*, and *Micrococcus luteus*, as well as the facultative bacterium *Escherichia coli*, were reacted with the $K_3Fe(CN)_6$/$K_4Fe(CN)_6$ reaction mixture under conditions similar to those adopted for *Actinobacter* spp. We did not observe the formation of magnetite even after 1 week of reaction. These control experiments clearly implicate the two inducible proteins secreted by *Actinobacter* spp. in the biotransformation of the ferri/ferrocyanide complexes into magnetite. Efforts are underway to purify and sequence these two proteins and test whether they show similarity with hydrolyzing proteins in magnetotactic bacteria and iron-reducing bacteria. The role of these inducible proteins in the metabolism of the bacterium will also be studied.

In conclusion, the bacterium, *Actinobacter* spp., has been shown to hydrolyze iron precursors to form iron oxide nanoparticles predominantly in the magnetite phase at room temperature. It is gratifying that this bacteria-driven biotransformation occurs under acidic and fully aerobic conditions, via a mechanism different from that observed in magnetotactic[9−12] and iron-reducing bacteria.[13] The simplicity of aerobic and room temperature synthetic routes for nanomagnetite over anaerobic synthesis together with the eco-friendly and energy-conserving nature of the process is an important advance.

Acknowledgment. We thank Prof. T. Enoki, TITECH Tokyo, Japan for assistance with low temperature field dependent magnetization measurements.

Supporting Information Available: Experimental details (S1) and TEM/SAED analysis of magnetite synthesized using the inducible proteins (S2) are available. This material is available free of charge via the Internet at http://pubs.acs.org.

References

(1) Corma, A. *Chem. Rev.* **1997**, *97*, 2373.
(2) Regan, B. O.; Gratzel, M. *Nature* **1991**, *353*, 737.
(3) Stoimenov, P. K.; Klinger, R. L.; Marchin, G. L.; Klabunde, K. J. *Langmuir* **2002**, *18*, 6679.
(4) Matsunaga, T. *Trends Biotechnol.* **1991**, *9*, 91.
(5) Raj, K.; Moskowitz, B.; Casciari, R. J. *Magn. Magn. Mater.* **1995**, *149*, 174.
(6) Lawaezeck, R.; Menzel, M.; Pietsch, H. *Appl. Organomet. Chem.* **2004**, *18*, 506.
(7) Matsunaga, T.; Okamura, Y.; Tanaka, T. *J. Mater. Chem.* **2004**, *14*, 2099.
(8) Hyeon, T. *Chem. Commun.* **2003**, 919.
(9) Blackmore, R. P. *Science* **1975**, *190*, 377.
(10) Bazylinski, D. A.; Frankel, R. B.; Jannusch, H. W. *Nature* **1988**, *334*, 518.
(11) Mann, S.; Frankel, R. B.; Blakemore, R. P. *Nature* **1983**, *310*, 405.
(12) Sakaguchi, T.; Burges, J. G.; Matsunaga, T. *Nature* **1993**, *365*, 47.
(13) Vali, H.; Weiss, B.; Li, Y.; Sears, S. K.; Kim, S. S.; Kirschvink, J. L.; Zhank, C. L. *Proc. Natl. Acad. Sci. U.S.A.* **2004**, *101*, 16121.
(14) Lane, D. J.; Pace, B.; Olsen, G. J.; Stahl, D. A.; Sogin, M. L.; Pace, N. R. *Proc. Natl. Acad. Sci. U.S.A.* **1985**, *82*, 6955.
(15) The XRD patterns were indexed with reference to the crystal structures from the *ASTM* charts: iron oxide [*ASTM* chart card no. 07−0322, 11−0614].
(16) Sorensen, C. M. In *Nanoscale Materials in Chemistry*; Klabunde, K. J., Ed.; Wiley: New York, 2002; p 169.
(17) Bala, T.; Bhame, S. D.; Joy, P. A.; Prasad, B. L. V.; Sastry, M. *J. Mater. Chem.* **2004**, *14*, 2941.

JA0508469